Case Studies in Construction Materials 16 (2022) e00778

Contents lists available at ScienceDirect

Case Studies in Construction Materials

journal homepage: www.elsevier.com/locate/cscm

Study of metakaolins with different amorphities and particle sizes activated by KOH and K_2SiO_3

Dayana Keitty Carmo Gonçalves [a,*], Sebastiana Luiza Bragança Lana [b], Rosemary Bom Conselho Sales [b], Maria Teresa Paulino Aguilar [c]

[a] Universidade Federal de Ouro Preto – UFOP, Brazil
[b] Universidade Estadual de Minas Gerais, UEMG, Brazil
[c] Universidade Federal de Minas Gerais - UFMG, Brazil

ARTICLE INFO

Keywords:
Geopolymerization
Amorphicity
Particle size, mechanical strength, water absorption

ABSTRACT

The study of alkaline activated materials is very promising regarding the production of materials with high durability. The particle size and the content of reactive silica e alumina (amorphous) influence the performance of the geopolymer as well as the type of activator. In this study, geopolymers are produced using metakaolin precursors with similar chemical composition and different amorphities and particle sizes. KOH and K_2SiO_3 are used as activators, therefore, potassium solutions provide a lower viscosity of the pastes, better workability with a lower liquid to solids ratio and, consequently, better mechanical strength, denser and exhibited low porosity than sodium solutions. Produced precursors and pastes were characterized in the solid state by fluorescence X-ray spectroscopy, X-ray diffraction, infrared spectroscopy, nuclear magnetic resonance single pulse and nuclear magnetic resonance cross-polarization. The pastes were also evaluated for compressive strength, bulk density and water absorption. The results indicate that geopolymers can be obtained from metakaolins of incomplete calcination and with average grain diameter of 23.5 μm and 12.0 μm. Despite having similar bulk density and a slight difference in water absorption, the mechanical strength of the paste produced with coarser and more amorphous metakaolin at 28 days is 50 MPa, while the other paste reaches 22 MPa. The difference in mechanical strength is likely due to the greater extent of geopolymerization indicated by the NMR. The difference in the precursors and consequently in the pastes impacts on the expected durability.

1. Introduction

The demand for durable materials is being researched around the world. These materials include alkali-activated compounds called geopolymers. These materials are obtained by the alkaline activation of minerals with a high silica and alumina and low calcium contents [1]. The range of applications for geopolymers is comprehensive and growing, allowing it to be used as a paste, mortar, reinforced concrete, matrices for the immobilization of hazardous, toxic and nuclear waste, among others [2–4].

Geopolymers have been widely used due to their high bending strength and compression strength, both in the early and late ages, resistance to high temperatures, including thermal insulation properties, stability to chemical attack (including acid), dimensional

* Corresponding author.
E-mail address: dayana.goncalves@aluno.ufop.edu.br (D.K.C. Gonçalves).

https://doi.org/10.1016/j.cscm.2021.e00778
Received 13 August 2021; Received in revised form 14 October 2021; Accepted 12 November 2021
Available online 17 November 2021

stability, strong adhesion to metallic and non-metallic surfaces, effective passivation of steel for structural reinforcement, low permeability to fluids and chloride ions, low cost, in addition to the possibility of incorporating industrial waste into the production chain [5,6]. However, studies show the performance of geopolymers, specially the durability of geopolymers is influenced by the type of precursors and activators used, variables that influence the extent of geopolymerization and the porosity of the mixture [7–12].

As a source of silica and alumina to be geopolymerized, natural rocks [13], industrial waste [14,15], agricultural waste [16] and metakaolin can be used. Of these, the most used as a precursor to produce geopolymers is metakaolin, which is obtained from the calcination of kaolin [17]. Depending on the calcination conditions, a metakaolin with different chemical compositions and atomic arrangements is obtained because the material is dehydroxylated during the process, making it amorphous. This situation was evidenced by the tetrahedral organization of Al and Si, which will foster geopolymerization [18]. According to the literature, for the extent of the geopolymerization reaction to be total, the precursor must be predominantly not crystalline, however regarding the influence of particle size the data are conflicting [19–22]. In the case of metakaolin, the necessity of grinding metakaolin to obtain a small size and kaolin calcination for higher times and temperatures can promote crystallization (mullite) in the kaolin.

Another factor influencing the geopolymerization reaction is the type of activator [23]. Sodium hydroxide and silicate are commonly used as alkaline activators. And silicates can be used to complementary sources of silica. However, other materials may also be used, including activators produced from agricultural or industrial waste [24,25]. Few studies use potassium [26,27]. Most studies on geopolymers use sodium hydroxide and silicate as activators, because sodium solutions are of low cost and it is possible to obtain good mechanical strength. Comparatively, mixtures using potassium activator require less liquid than sodium-based activations to achieve the same workability, since potassium solutions have lower viscosity than sodium solutions [28]. The reactivity of the components and the consequent compressive strength is also higher when using potassium activators [29]. In addition, potassium solutions lead to a lower initial viscosity. This is due to the size of its hydration radius and consequently the greater number of H_2O molecules associated with the K^+ ion [30]. As for the setting time using potassium activators, it is shorter than when using sodium. Rocha et al. [31] obtained similar strength using sodium and potassium activators. However, mortars produced with alkaline sodium silicate exhibited a heterogeneous microstructure with many pores, while those containing potassium silicate were denser and exhibited low porosity. Thus, it is expected that pastes produced with potassium-based solutions demand a lower water to solids ratio and, consequently, present greater mechanical strength, as well as greater durability due to the microstructure with fewer pores. However, the cost of producing potassium-based mixtures is higher than for sodium mixtures [28].

In this sense, this work evaluates the extent of geopolymerization in metakaolin with different amorphities and coarse particle sizes using a mixed solution of K2SiO3 and KOH as activators. The relationship between the compressive strength and porosity evaluates by the bulk density and percentage of water absorption is analyzed, with the objective of relating durability and characteristics of the precursor material.

2. Experimental procedure

Geopolymeric pastes (P1 and P2) were produced using two types of metakaolin (M1 and M2), both available on the market, at mass ratio 1:1 (precursor: activator solution). The alkaline solution was potassium silicate (K_2SiO_3) and potassium hydroxide (KOH) at ratio 2:1 (K_2SiO_3: KOH). The potassium hydroxide solution was prepared with 10 M. The composition was fixed with the aim of creating an alkaline environment with a sufficient supply of silica and alumina [32]. After activation, the pastes were kept a temperature of approximately 25ºC until the date of the experiments.

In the chemical characterization of metakaolin, X-ray fluorescence spectroscopy (XRF) was used. The samples were prepared by fusion with lithium tetraborate. The particle size of the precursor was evaluated by laser beam scattering using a CILAS 1090 particle size meter. The structure of the atomic arrangement and the nature of the constituents in the precursors and pastes were evaluated by X-ray diffraction (XRD) and Fourier transform infrared spectroscopy (FTIR). For the XRD, a Shimadzu XRD-7000 diffractometer with a copper tube, a scanning angle 10–120º and a step of 0.02 s^{-1} was used. The FTIR analysis was performed using a Nicolet 6700 - Thermo Scientific DRIFTS mode -, diffuse reflectance, covering the range 4.000–500 cm^{-1}, with a resolution of 4 cm^{-1}, and 64 scans.

The coordination of Al and Si in metakaolin and pastes was assessed by solid state nuclear magnetic resonance spectroscopy (NMR). The Bruker Avance 600 MHz equipment, with a field of 14.1 Tesla, was used to detect Al^{27} at 156.38 MHz by simple pulse analysis with a magic angle rotation in 4-mm rotors rotating at 13.5 kHz, 15 s repetition time, 16 scans, and 2.3 μs pulse. The NMR test for Si^{29} detection was performed on a Bruker 400 DSX equipment with a 9.4 Tesla field and a 79.49 MHz frequency using single-angle pulse techniques on 7-mm rotors rotating at 6.5 kHz, repeating time 900 s, 24 sweeps, and 8 μs pulse. Cross-polarization assays with "magic angle" rotation were also performed, in these cases 2 ms repetition time, 512 scans, and 12.2 μs pulse. Both geopolymer pastes and precursors were analyzed under the same conditions.

The bulk density, water absorption and compressive strength of the pastes were determined using as a reference standardization

Table 1
XRF - Chemical composition of metakaolins M1 and M2.

	Oxide (%)								
Metakaolin	Al_2O_3	SiO_2	CaO	Fe_2O_3	K_2O	Na_2O	MgO	MnO	TiO_2
M1	42.80	53.90	0.06	0.39	0.76	< 0.10	0.34	0.01	0.03
M2	45.10	53.40	0.04	0.24	0.10	< 0.10	0.23	< 0.01	0.05

applied to Portland cement products [33,34]. The compressive strengths were evaluated at 6 h, 24 h, 7 days and 28 days after molding and the other two properties at 28 days.

3. Results and discussion

Table 1 shows the chemical composition of the major oxides present in the precursors obtained by XRF. Both metakaolins have high levels of Al_2O_3 and SiO_2. The levels of CaO and Fe_2O_3 are lower than 1% in both metakaolins. At high concentrations, there is the possibility of replacement of Al in the geopolymeric network for Ca and Fe [35]. According to Buchwald [36] and Lolli et al. [37], the chemical composition has a strong influence on the final strength of the material in geopolymers, specially ratio SiO_2/Al_2O_3. This ratio must be greater than 1 in materials with the potential to be geopolymer precursors, as Al is present only in this material. For each silicate tetrahedron, at least one aluminate is required, as silicates dissolve in water. Santa [32] indicates the ideal ratio for pastes is between 3.0 e 4.5. Ratio SiO_2/Al_2O_3 in both precursors is 2.0. Using the mixed potassium hydroxide and silicate activating solution, ratio SiO_2/Al_2O_3 in both pastes is 3.0, because the soluble silica present in the silicate solution contributes to the increase in this ratio. This relation is important because it affects the hardening and mechanical strength.

Related to the particle size, it is possible to notice a greater uniformity in metakaolin M2 (Fig. 1). In metakaolin M1, the particle size distribution is more heterogeneous. The particle size distribution affects the properties of the pastes as it promotes packaging. Therefore, it changes the rheological properties of the material during the mixing process and in the case of non-reactive particles mechanical properties of the hardened material. The mean grain diameter in the metakaolin M1 is 12.0 μm and in M2 is 23.5 μm. M1 and M2 metakaolins have 90% of the particles with a diameter smaller than 30.0 μm and 50.8 μm, respectively. Based on this, it can be considered that M1 has a smaller particle size. Thus, when it comes to grain size, a higher reactivity of metakaolin M1 is expected compared to the metakaolin M2 [20].

In metakaolin diffractograms (Fig. 2), the presence of a curved region (halo) formed by the deviation from the baseline at $2\theta = 18–30^\circ$ can be attributed to amorphous aluminosilicates [19,38]. The precursor M1 presents visually a lower amorphity compared to the precursor M2. According to Lolli et al. [37], it is expected that the greater the amorphity, the greater the extent of geopolymerization. The diffraction peaks detected in both precursors indicate the existence of crystalline phases such as quartz, muscovite and kaolinite. The presence of kaolinite may be related to incomplete calcination and quartz may be related to kaolin impurities [18]. This means a smaller content of amorphous (reative) silica available.

In both geopolymer pastes (Fig. 2), there is a halo corresponding to the existence of an amorphous phase between $2\theta = 20–35^\circ$, which is offset from the metakaolin ($2\theta = 18–30^\circ$). This change has been associated with the formation of new amorphous phases. It is indicative of a geopolymeric reaction [39]. The crystalline peaks in the precursors remained in the pastes. This indicates that the solution is not able to disorganize all of the crystalline phases present in the precursors. These phases are being able to act as filling material in the pastes. However, the crystalline content of the pastes in relation to the precursors, decreased, indicating that part of the crystalline materials was part of the geopolymerization reaction.

Fig. 3 shows the infrared absorption bands of the precursors and pastes obtained by Fourier transform infrared spectroscopy (FTIR). It is possible to observe characteristic bands of free water (capillary and adsorbed) in both the precursor and the pastes. It is more evident in the pastes in relation to the precursors: the band is approximately 1650 cm^{-1}. In pastes, an absorption band of approximately 3440 cm^{-1} is observed. This is characteristic of water trapped in cavities or absorbed due to the geopolymerization process [40].

In the paste produced using the precursor M2 (Fig. 3), it is possible to note a band at approximately 1395–1510 cm^{-1}, which indicates a carbonation process. This process could be attributed to the formation of carbonates from the unreacted hydroxide present in the activator interacted the carbon dioxide of the atmosphere.

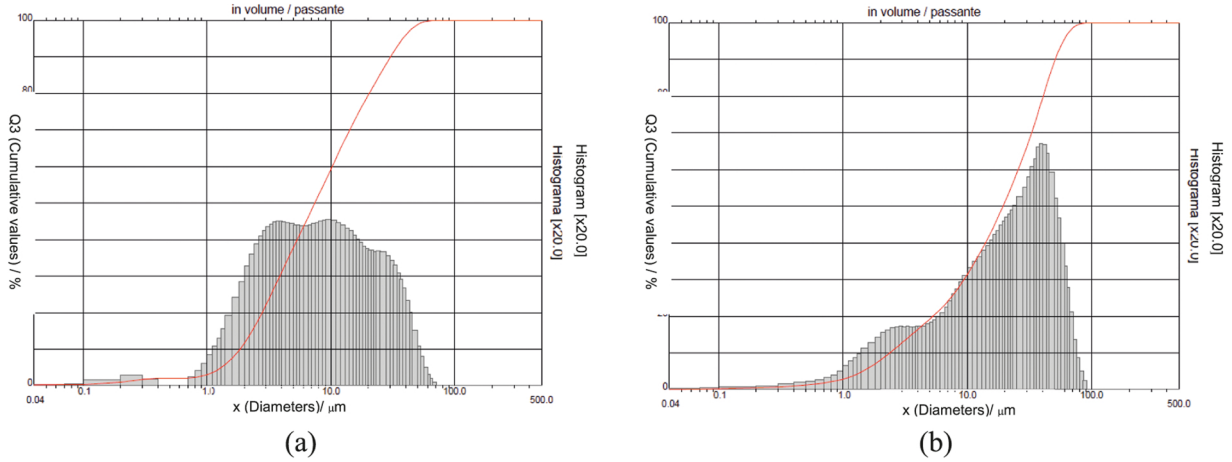

Fig. 1. Particle size distribution (a) M1 precursor and (b) M2 precursor.

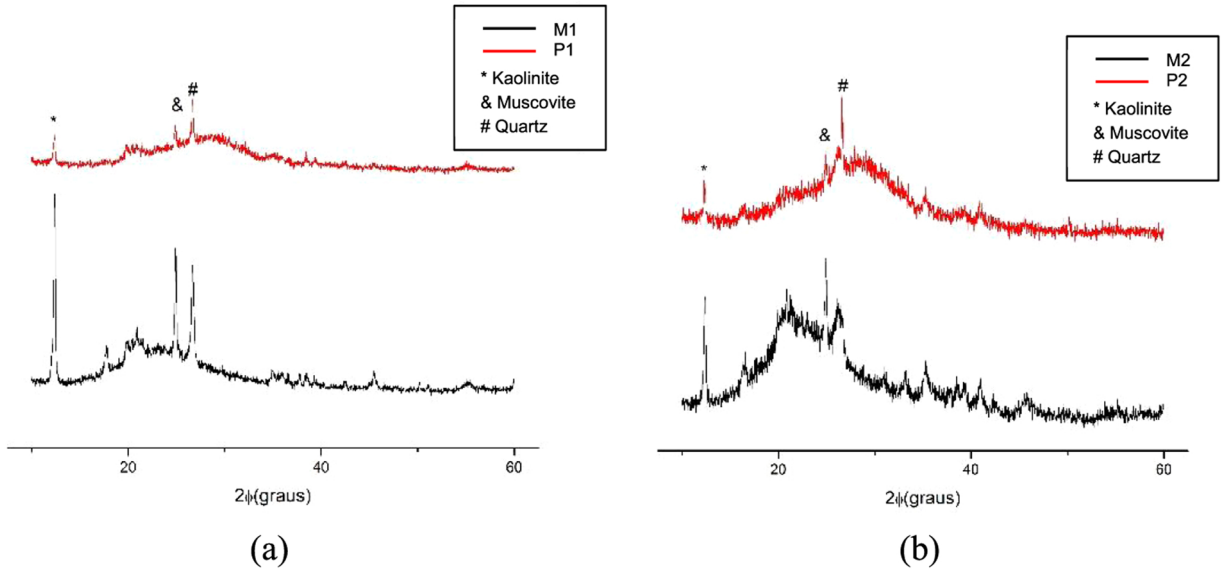

Fig. 2. XRD of the metakaolin and the paste (a) Precursor M1 and Paste P1 and (b) Precursor M2 and Paste P2.

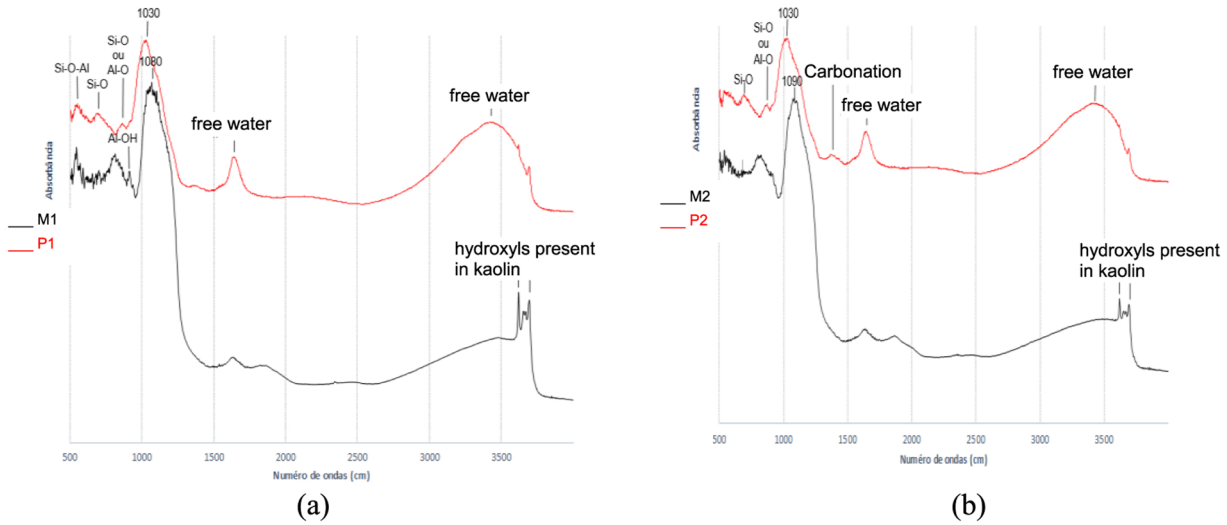

Fig. 3. FTIR of the metakaolin and the paste (a) Precursor M1 and Paste P1 and (b) Precursor M2 and Paste P2.

It is possible to observe (Fig. 3) the band with a maximum point around 1030–1010 cm^{-1} in both pastes, while these values are around 1090–1065 cm^{-1} in the precursors. The displacement of the band is clear. The bands that appear at 1010 and 1030 cm^{-1} are due to Si–O bonds [41]. The band from 1065 to 1090 cm^{-1} is characteristic of the Si-O-Al stretch vibration [40,42].

In the spectrogram, it is also possible to observe the band at approximately 950 cm^{-1}. This band appears due to the reorganization of AlO_4 or SiO_4 resulting from the geopolymerization process and resulting in Si-O-Si or Al-O-Si [38]. The absorption band present especially in the precursors at approximately 915–910 cm^{-1} is attributed to the stretching of Al-OH in tetrahedral coordination [40, 42]. The bands observed in the materials within the range 800–500 cm^{-1} are all due to bending vibrations of Al-O-Si. Bands at approximately 540 cm^{-1} indicate the presence of off-plane folding of Si-O specimens [40,41].

Fig. 4 shows the Al^{27} spectra obtained by NMR for the precursors and pastes. Three signals are observed in the precursor materials at approximately 4 ppm (AlO_6), at 29 ppm (AlO_5), and at 50 ppm (AlO_4) [43,44]. The presence of signals related to the tetrahedral coordinates Al (IV) and the pentahedral sites Al (V) agrees with the calcination and metakaolin formation process. However, the intense Al (VI) signal indicates that the calcination was not total, still existing kaolinite. The amorphous phases Al (IV) and Al (V) are highly reactive, facilitating the precursor reaction to geopolymer formation despite the presence of kaolinite. There are side bands due to the rotation in the "magic angle." For the precursor M2, there is a greater Al (IV) intensity at 57 ppm than Al (V) at 29 ppm. Furthermore, in this precursor, a signal at approximately 12 ppm is observed, which can be attributed to noise. Compared to the

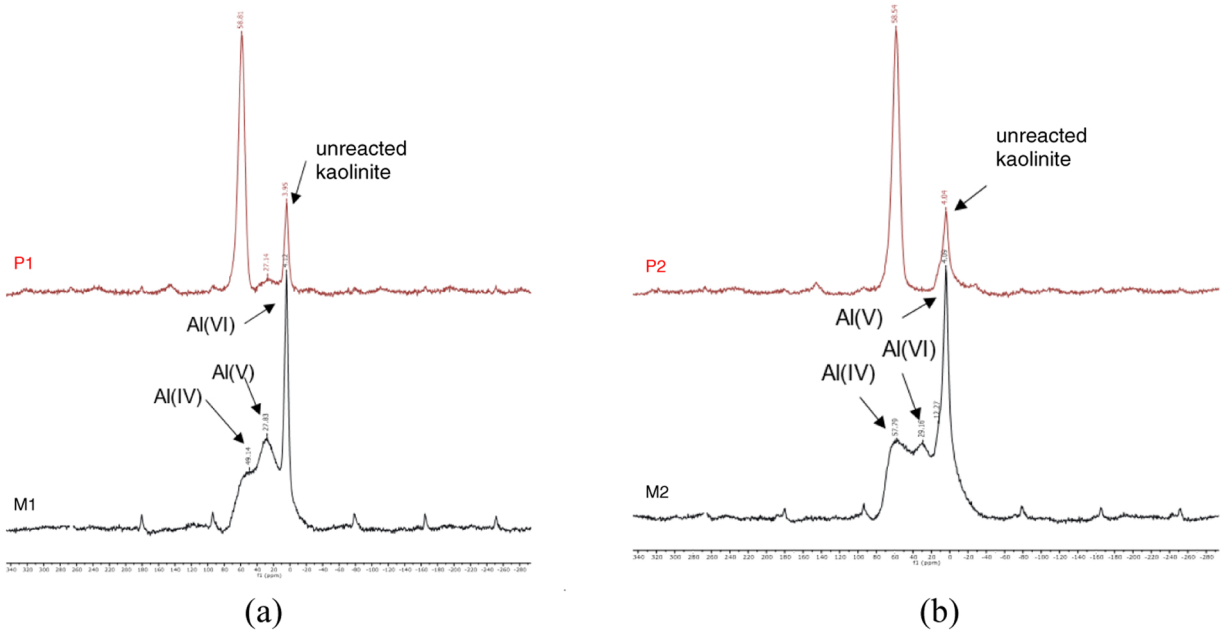

Fig. 4. NMR of metakaolin and paste in the state of Al^{27} (a) Precursor M1 and Paste P1 and (b) Precursor M2 and Paste P2.

precursor M2, the precursor M1 had more Al (V), which is not reactive.

Fig. 5 shows the Si^{29} spectra obtained by NMR for the precursors and pastes by the single pulse technique. The geopolymerization process can be seen in pastes as it has a significant peak within the range that characterizes tetrahedral coordination. A peak of approximately 5 ppm is also identified. It can be attributed to the presence of kaolinite in both pastes.

It is possible to observe that the precursor M1 (Fig. 5) showed signals around −106 ppm and −91.2 ppm. The signal close to −91.2 ppm is assigned to layered silicates originating from kaolin [43,44] and represents a Si core bonded to three other silicones by Q_3 covalent bonds. After calcination, the crystallinity is expected to be lower and, therefore, the material has a single component at approximately −106 ppm, a signal attributed to a Si core linked to four another Si (Q_4), also present in the sample but less intensely. The signal width indicates that this is an amorphous structure and that it was formed at kaolinite calcination. However, both precursors behave similarly with signals around −106 ppm and 91.19 ppm. In the metakaolin M2, it is possible to observe a greater formation of the Si Q_4 structure, which is reactive (Fig. 5). The line present at approximately −76 ppm can be attributed to assay noise.

In paste P1, it is also possible to note signal disappearance at approximately −106 ppm and the appearance of the signal at −86.5 ppm. This behavior indicates the consumption of Q_4 structures during geopolymerization with the formation of Q_3 structures, indicating the extent of geopolymerization.

In paste P2, a higher peak intensity is observed regarding the tetrahedral structures, indicating a greater extension of the geopolymeric network. As expected, the signal at −91.1 ppm was still present. A signal widening centered at 91.1 ppm indicates the formation of a new Q_3 structure, probably of amorphous character, and the considerable decrease in the signal at −106 ppm indicates that Q_4 units have been consumed or reacted.

Fig. 6 shows the solid-state NMR spectrum of Si^{29} of the precursor and the paste using the cross-polarization technique. In both pastes, as expected, signals at approximately −91 ppm, probably referring to unreacted kaolinite in the process of calcination and geopolymer formation, remain present. However, after geopolymerization, a signal enlargement process is observed, indicating the formation of a new Q_3 structure, probably of amorphous character, since the process is accompanied by a signal decrease of approximately −106 ppm, which indicates the consumption or reaction of Q_4 units. In addition, in the cross-polarization spectrum beyond the kaolinite signal, another spectrum was also observed at −86.8 ppm, which probably refers to the Q_3 structure.

Table 2 shows the bulk density and water absorption for both pastes` 28 day-cure. Although the bulk density was the same in both pastes, in the water absorption test a difference of 8% was found. This would indicate a slightly greater open porosity of the P2 paste, obtained from a metakaolin with higher particle size [21], which would provide less resistance to fluid penetration, which could compromise the durability of the paste.

Fig. 7 shows the evolution of compressive strength in relation to cure time (6 h to 28 days). It is observed that, in 24 h, the P1 paste reaches around 85% of the strength obtained at 28 days. In the P2 paste, the growth of the compressive strength is monotonic, with a deceleration after the first 24 h, which corresponds, at this age, to about 35% of the strength obtained at 28 days. It is noticed that the reaction speed of both pastes is similar in the first 24 h. This indicates that the particle size difference is not strongly affected the reaction kinetics in the dissolution step [22,45]. However, as it is less amorphous, metakaolin M1 has lower levels of reactive silica and alumina, which are exhausted in the early ages, a stabilization occurring in the compression strength with this paste (P1). This inference is evidenced by the NMR results, which indicated the lower content of reactive material in M1 and, consequently, a smaller

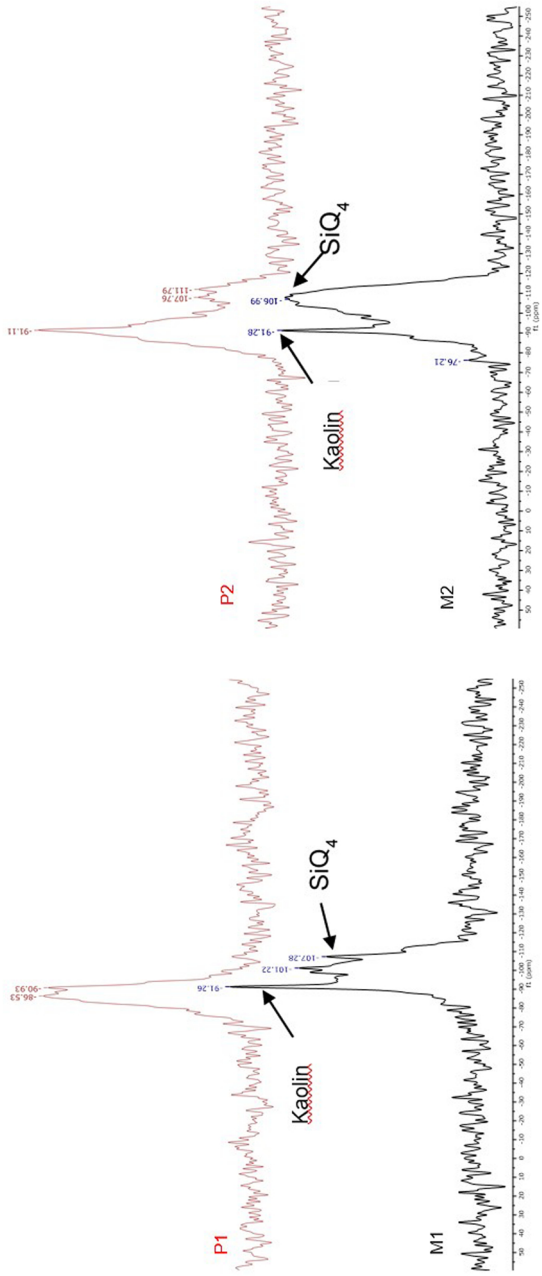

Fig. 5. NMR of the metakaolin and paste in the Si^{29} state by single pulse (a) Precursor M1 and Paste P1 and (b) Precursor M2 and Paste P2.

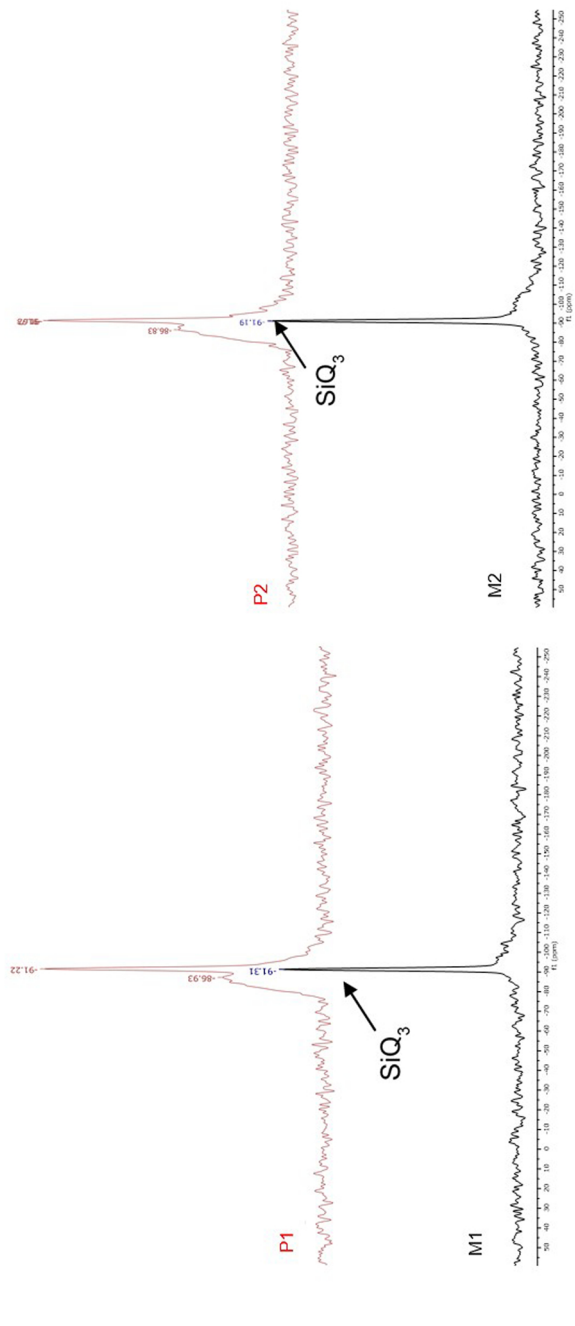

Fig. 6. NMR of metakaolin and paste in the state of Si^{29} using the cross-polarization technique (a) Precursor M1 and Paste P1 and (b) Precursor M2 and Paste P2.

Table 2
Bulk density and water absorption.

	Bulk density (g/cm^3)	Water absorption (%)
P1	2.70	21.5
P2	2.66	28.5

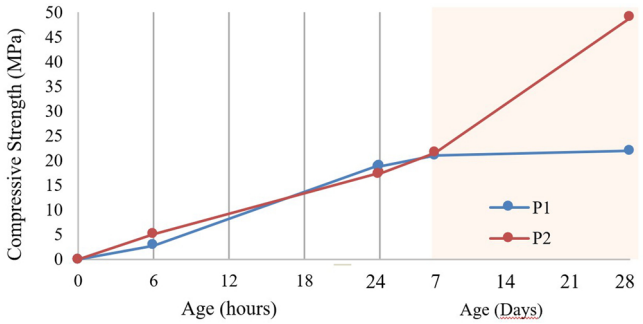

Fig. 7. Compressive Strength.

extent of geopolymerization in P1 than in P2. However, if M1 and M2 had been properly calcined, a better extension of geopolymerization and consequent better performance would be possible.

The fact that both pastes present the same bulk density and different compressive strengths at 28 days, may be related to the presence of non-reactive (crystalline) and, therefore, non-resistant silica and alumina in the P1 paste. These materials probably acted as fillers, influencing the density and compensating for the lack of geopolymerized product. The difference in water absorption may be related to the greater size and connectivity of the pores in P2 due to the use of a precursor of greater particle size. This situation may indicate a greater resistance to fluid penetration in P1 than in P2.

The increase in strength after initial ages in both pastes, is indicative of maintaining the bearing capacity of the geopolymers with age. The occurrence of a decrease in resistance after the first ages is reported in studies in the literature and compromises the durability of the compounds. The phenomenon is related to the breaking of Si-O-Si (Q_4) bonds by activator ions, with the formation of Si-O-M+ bonds, Non-bridging Oxygens, which would be evidenced even in the NMR by an increase in presence of type Q_2 specimens, a situation that does not occur with the evaluated pastes [46–48].

4. Conclusion

The precursor analyses indicate that the calcination for obtaining metakaolins is incomplete. It was possible to identify kaolinite using XRD and hydroxyl groups present in kaolin using FTIR, and Al (VI) using NMR. In the case of the precursor M2, it is possible to observe a greater amorphity, which could indicate a more efficient calcination. As for particle size, M1 has an average diameter around 51% smaller than M2. The analyses of pastes indicate that the mixed activator KOH and K_2SiO_3 promoted the geopolymerization of metakaolins of incomplete calcination and coarse particle size. In paste P2 the greater extension of the geopolymeric network was observed by the NMR. Both pastes had the same bulk density, but P2 had a slightly higher water absorption, that is, greater open porosity and, consequently, lower resistance to fluid penetration.

The compressive strength as well as its evolution with the age of the pastes, varied significantly with the type of metakaolin used, especially about the degree of amorphicity, since the reaction rate in the first ages was similar for both pastes. The paste obtained with the less amorphous precursor showed 45% lower strength at 28 days, probably because of the worse extension of geopolymerization. The particle fraction appears to have no effect on the mechanical strength.

The fact that both pastes have the same bulk density and compressive strengths at 28 different days may be related to the presence of non-reactive silica and alumina in the P1 paste, which would act as a filler and compensate in terms of mass for the lack of resistant product in the geopolymer. The higher percentage of water absorption of the P2 paste may be related to the greater dimension and connectivity of the pores, due to the use of a precursor of greater granulometry. Thus, despite being more mechanically resistant, P2 tends to have lower resistance to fluid penetration, which can impact the performance of the paste.

After the first ages, no decay of compressive strength was observed in both geopolymers, indicating the non-occurrence of O-Si-M^+ bonds, which are harmful to the material's performance.

Declaration of Competing Interest

The authors declare that they have no known competing financial interests or personal relationships that could have appeared to influence the work reported in this paper.

Acknowledgments

To CAPES (Coordination for the Improvement of Higher Education Personnel), Brazil, to CNPq (Council National Scientific and Technological Development), Brazil, to FAPEMIG (Foundation for the Support of Minas Gerais State Survey), Brazil and the BAM (Federal Institute for Materials Research and Testing), Germany, for supporting the study.

References

[1] K. Neupane, D. Chalmers, P. Kidd, High-strength geopolymer concrete - properties, advantages and challenges, Adv. Mater. 7 (2) (2018) 15.
[2] E. Barrie, V. Cappuyns, E. Vassilieva, R. Adriaens, S. Hollanders, D. Garcés, L. Machiels, Potential of inorganic polymers (geopolymers) made of halloysite and volcanic glass for the immobilization of tailings from gold extraction in Ecuador, Appl. Clay Sci. (2015).
[3] T. Luukkonen, A. Heponiemi, H. Runtti, J. Pesonen, J. Yliniemi, U. Lassi, Application of alkali-activated materials for water and wastewater treatment: a review, Rev. Environ. Sci. Bio/Technol. (2019).
[4] A. Palomo, P. Krivenki, I. Garcia-Lodeiro, E. Kavalerova, O. Maltseva, A. Fernández-Jiménez, A review on alkaline activation: new analytical perspectives, Mater. de Constr. 64 (315) (2014).
[5] J.L. Provis, S.A. Bernal, Geopolymers and related alkali-activated materials, Annu. Rev. Mater. Res. 44 (1) (2014) 299–327.
[6] M.T. Marvila, A.R.G. Azevedo, G.C.G. Delagua, B.C. Mendes, L.G. Pedroti, C.M.F. Vieira, Performance of geopolymer tiles in high temperature and saturation, Constr. Build. Mater. 286 (2021).
[7] T. Lingyu, H. Dongpo, Z. Jianing, W. Hongguang, Durability of geopolymers and geopolymer concretes: a review, Rev. Adv. Mater. Sci. 60 (1) (2021) 1–14.
[8] A.R.G. De Azevedo, M. Teixeira Marvila, L. Barbosa de Oliveira, W. Macario Ferreira, H. Colorado, S. Rainho Teixeira, C. Mauricio Fontes Vieira, Ciruclar economy and durability in geopolymers ceramics pieces obtained from glass polishing waste, Int. J. Appl. Ceram. Technol. (2021).
[9] M.T. Marvila, A.R.G. d Azevedo, P.R. d Matos, S.N. Monteiro, C.M.F. Vieira, Rheological and the fresh state properties of alkali-activated mortars by blast furnace slag, Materials 14 (8) (2021).
[10] T. Bakharev, Resistance of geopolymer materials to acid attack, Cem. Concr. Res. 35 (4) (2005) 658–670.
[11] T. Bakharev, Durability of geopolymer materials in sodium and magnesium sulfate solutions, Cem. Concr. Res. 35 (6) (2005) 1233–1246.
[12] M. Zhang, G. Zhao, D. Zhang, K. Mann, K. Lumsden, M. Tao, Durability of red mud-fly ash based geopolymer and leaching behavior of heavy metals in sulfuric acid solutions and deoionized water, Constr. Build. Mater. 124 (2016) 373–382.
[13] J.M. Dassekpo, X. Zha, J. Zhan, Compressive strength performance of geopolymer paste derived from completely decomposed granite (CDG) and partial fly ash replacement, Constr. Build. Mater. 138 (2017) 195–203.
[14] A. Fernández-Jiménez, A. Palomo, M. Criado, Microstructure development of alkali-activated fly ash cement: a descriptive model, Cem. Concr. Res. 35 (2005) 1204–1209.
[15] A.R.G. De Azevedo, M. Teixeira Marvila, H.A. Rocha, L.R. Cruz, C.M.F. Vieira, Use of glass polishing waste in the development of ecological ceramic roof tiles, Int. J. Appl. Ceram. Technol. (2020).
[16] P. Sturm, G.J.G. Gluth, H.J.H. Brouwers, H.-C. Kuhne, Synthesizing one-part geopolymers from rice husk ash, Constr. Build. Mater. 124 (2016) 961–966.
[17] J. Davidovits, Geopolymer Based on Natural and Synthetic Metakaolin a Critical Review, in: Proceedings of the 41st International Conference on Advanced Ceramics and Composites, p. 201, 2018.
[18] C.M.G. de Souza, S. Greiser, E. Garcia, V.A. Quarcioni, C. Jager, Evaluation of pozzolanic reactivity of calcined kaolinite, Int. J. Res. Eng. Technol. 3 (2014) 209–213.
[19] P. Duxson, A. Fernández-Jiménez, J.L. Provis, G.C. Lukey, Geopolymer technology: the current state of the art, J. Mater. Sci. 42 (9) (2007) 2917–2933.
[20] H. Rahier, J.F. Denayer, B. Van, Mele, Low-temperature synthesized aluminosilicate glasses Part IV Modulated DSC study on the effect of particle size of metakaolinite on the production of inorganic polymer glasses, J. Mater. Sci. 38 (14) (2003) 3131–3136.
[21] L.N. Assi, E. Eddie Deaver, P. Ziehl, Effect of source and particle size distribution on the mechanical and microstructural properties of fly ash-based geopolymer concrete, Constr. Build. Mater. 167 (2018) 372–380.
[22] J. Zhang, S. Li, Z. Li, C. Liu, Y. Gao, Feasibility study of red mud for geopolymer preparation: effect of particle size fraction, J. Mater. Cycles Waste Manag. 22 (5) (2020) 1328–1338.
[23] M.T. Marvila, A.R.G. Azevedo, C.M.F. Vieira, Reaction mechanisms of alkali-activated materials, Rev. IBRACON de Estruturas e Mater. 14 (3) (2021).
[24] J.L. Provis, J.S.J. Van Deventer, Alkali Activated Materials: State-of-the-art Report, Springer Science & Business Media, 2013.
[25] B.C. Mendes, L.G. Pedroti, C.M.F. Vieira, M. Marvilla, A.R.G. Azevedo, J.M.F. Franco, J.C.L. Ribeiro, Application of eco-friendly alternative activators in alkali-activated materials: a review, J. Build. Eng. (2020).
[26] X. Ke, J.L. Provis, S.A. Bernal, Structural Ordering of Aged and Hydrothermally Cured Metakaolin Based Potassium Geopolymers (in Calcined Clays for Sustainable Concrete), Springer, Dordrecht, 2018, pp. 232–237 (in Calcined Clays for Sustainable Concrete).
[27] K. Keshari, M. Manish, K.C. Ramesh, B. Abhishek, Feasibility studies for development of cement free fly ash based geo-polymer mortar using potassium based alkaline activator, Int. Res. J. Eng. Technol. 5 (4) (2018) 3334–3338.
[28] D. Sabitha, J.K. Dattatreya, N. Sakthivel, M. Bhuvaneshwari, S.A. Jaffer Sathik, Reactivity, workability and strength of potassium versus sodium-activated high volume fly ash-based geopolymers, Curr. Sci. 103 (11) (2012) 1320–1327.
[29] M. Lizcano, H.S. Kim, S. Basu, M. Radovic, Mechanical properties of sodium, J. Mater. Sci. 47 (2012) 2607–2616.
[30] J.L. Provis and J.S. J. Van Deventer, Geopolymers: Structures, Processing, Properties and Industrial Applications, 2009.
[31] T. d S. Rocha, D.P. Dias, F.C.C. França, R.R. d S. Guerra, L.R. d C. d O. Marques, Metakaolin-based geopolymer mortars with different alkaline activators (Na+ and K+), Constr. Build. Mater. 178 (2018) 453–461.
[32] R.A. A.B. Santa, Síntese de geopolímeros a partir de cinzas pesadas e metacaulim para avaliação das propriedades de solidificação/imobilização de resíduos tóxicos, 2016.
[33] A.-A. B. d.N. Técnicas, NBR 9778:2005 Hardened mortar and concrete - Determination of absorption, voids and specific gravity, 2005.
[34] A.-A. B. d.N. Técnicas, NBR 5739:2018 Concrete - Compression test of cylindrical specimens, 2018.
[35] R.C. Kaze, L.M. Beleuk à Moungam, M.L. Fonkwe Djouk, A. Nana, E. Kamseu, U.F. Chinje Melo, C. Leonelli, The corrosion of kaolinite by iron minerals and the effects on geopolymerization, Appl. Clay Sci. 138 (2017) 48–62.
[36] A. Buchwald, What are geopolymers? Current state of research and technology, the opportunities they offer, and their significance for the precast industry, Betonwerk++ Fertigteil-Technik 72 (7) (2006).
[37] F. Lolli, H. Manzano, J.L. Provis, M. Bignozzi, Atomistic simulations of geopolymer models: the impact of disorder on structure and mechanics, ACS Appl. Mater. Interfaces 10 (26) (2018) 22809–22820.
[38] J.L. Provis, J.S.J. Van Deventer, Geopolymers: Structures, Processing, Properties and Industrial Applications, Elsevier, 2009.
[39] J. Davidovits, Geopolymer Cement. A Rewiew, Geopolymer Institute, Saint-Quentin, France, 2013.
[40] M. Catauro, F. Papale, G. Lamanna, F. Bollino, Geopolymer/PEG hybrid materials synthesis and investigation of the polymer influence on microstructure and mechanical behavior, Mater. Res. 18 (4) (2015) 698–705.
[41] M. Król, P. Rożek, D. Chlebda, W. Mozgawa, Influence of alkali metal cations/type of activator on the structure of alkali-activated fly ash – ATR-FTIR studies, Spectrochim. Acta Part A: Mol. Biomol. Spectrosc. 198 (2018) 33–37.
[42] J. Davidovits, Geopolymers - Chemistry and Applications, Institute Géopolymére, Saint-Quentin, 2008.

[43] A.C. El Idrissi, M. Paris, E. Roziere, D. Deneele, S. Darson, A. Loukili, Alkali-activated grouts with incorporated fly ash: From NMR analysis to mechanical properties, Mater. Today Commun. 14 (2018) 225–232.
[44] P. Duxson, The structure and thermal evolution of metakaolin geopolymers, 2006.
[45] M. Najimi, N. Ghafoori, M. Sharbaf, Alkali-activated natural pozzolan/slag mortars: a parametric study, Constr. Build. Mater. 164 (2018).
[46] R.A.M. Figueiredo, P.R.G. Brandão, M. Soutsos, A.B. Henriques, A. Fourie, D.B. Mazzinghy, Producing sodium silicate powder from iron ore tailings for use as an activator in one-part geopolymer binders, Mater. Lett. 288 (2021).
[47] P.I.K. Onorato, M.N. Alexander, C.W. Struck, G.W. Tasker, D.R. Uhlmann, Bridging and nonbridging oxygen atoms in alkali aluminosilicate glasses, J. Am. Ceram. Soc. 68 (6) (1985) C–148-C-150.
[48] D.M. Zirl, S.H. Garofalini, Structure of sodium ahminosilicate glass surfaces, J. Am. Ceram. Soc. 75 (9) (1992) 2353–2362.